




# LAPTM5 mediates immature B cell apoptosis and B cell tolerance by regulating the WWP2-PTEN-AKT pathway

Ying Wang<sup>a,1</sup>, Jun Liu<sup>a,1</sup>, Chizuru Akatsu<sup>b</sup>, Runyun Zhang<sup>a</sup>, Hai Zhang<sup>c</sup>, Han Zhu<sup>d</sup>, Kangwei Liu<sup>d</sup>, Han-Ying Zhu<sup>a</sup>, Qing Min<sup>e</sup>, Xin Meng<sup>a</sup>, Chaoqun Cui<sup>a</sup>, Yue Tang<sup>a</sup>, Meiping Yu<sup>f</sup>, Yaxuan Li<sup>a</sup>, Xiaoqian Feng<sup>a</sup>, Hao Wei<sup>a</sup>, Zichao Wen<sup>a</sup>, Sihan Ji<sup>a</sup>, Martin G. Weigert<sup>g</sup>, Takeshi Tsubata<sup>b</sup>, and Ji-Yang Wang<sup>a,c,f,g,h,2</sup> 

Edited by Max Cooper, Emory University, Atlanta, GA; received March 31, 2022; accepted July 1, 2022

**Elimination of autoreactive developing B cells is an important mechanism to prevent autoantibody production. However, how B cell receptor (BCR) signaling triggers apoptosis of immature B cells remains poorly understood. We show that BCR stimulation up-regulates the expression of the lysosomal-associated transmembrane protein 5 (LAPTM5), which in turn triggers apoptosis of immature B cells through two pathways. LAPTM5 causes BCR internalization, resulting in decreased phosphorylation of SYK and ERK. In addition, LAPTM5 targets the E3 ubiquitin ligase WWP2 for lysosomal degradation, resulting in the accumulation of its substrate PTEN. Elevated PTEN levels suppress AKT phosphorylation, leading to increased FOXO1 expression and up-regulation of the cell cycle inhibitor p27Kip1 and the proapoptotic molecule BIM. In vivo, LAPTM5 is involved in the elimination of autoreactive B cells and its deficiency exacerbates autoantibody production. Our results reveal a previously unidentified mechanism that contributes to immature B cell apoptosis and B cell tolerance.**

B cell tolerance | immature B cell | apoptosis | lysosomal-associated transmembrane protein 5 | E3 ubiquitin ligase

B cell development is a process of sequential immunoglobulin (Ig) heavy chain (HC) and light chain (LC) gene rearrangements (1). Early B cells with successful rearrangements of both HC and LC genes become immature B cells that express a membrane IgM B cell receptor (BCR). Due to the random nature of rearrangements, it has been estimated that as many as 85% of the newly generated immature B cells can recognize self-antigens (2). To prevent autoantibody production by such autoreactive B cells, the immune system has developed multiple mechanisms, including B cell central and peripheral tolerance, to eliminate/inactivate autoreactive B cells. B cell central tolerance functions to remove autoreactive immature B cells in the bone marrow (BM) by at least three mechanisms: 1) clonal deletion via apoptosis of immature B cells that recognize self-antigens with high avidity; 2) alternatively, such immature B cells may initiate a new round of light chain rearrangement, a process called receptor editing, to change the specificity of the BCR; and 3) immature B cells that recognize self-antigens with low avidity may become functionally unresponsive or anergic, due to the down-modulation of BCR expression/signaling (3, 4). Immature B cells that escape central tolerance can also become anergic by repeated stimulation of self-antigens in the absence of T cell help. In addition, self-reactive B cells can also be generated during T-dependent B cell response in the germinal centers and can be eliminated by the interaction of FAS on the activated B cells with FASL on helper T cells (5). Defects in central or peripheral tolerance can lead to autoimmune diseases manifested by increased autoantibody levels, inflammation, and tissue damage (6, 7). Hitherto, a number of genes have been implicated in the elimination of autoreactive immature B cells (3), including *Bcl-2* (8), *Pik3* (9–11), *Pten* (12, 13), *Aicda* (14), and miR-148a (15). However, the precise molecular mechanisms have remained incompletely understood.

B cell tolerance has been investigated in several animal models. Using mice transgenic for a heavy and a light chain specific for the H-2K<sup>k</sup> MHC molecule, it has been shown that B cells developed and matured normally in mice with H-2K<sup>d</sup> background, but were undetectable in mice expressing H-2K<sup>k</sup>, suggesting that immature B cells bearing the autoreactive BCR were deleted. It was also found that in mice with both H-2K<sup>d</sup> and H-2K<sup>k</sup> MHC, some of the autoreactive B cells were not deleted but instead underwent light chain receptor editing and no longer bound to the H-2K<sup>k</sup> antigen (16, 17). Using double-transgenic mice expressing membrane hen egg lysozyme (mHEL) and anti-HEL BCR, it was shown that B cells in these mice underwent efficient clonal deletion, with few B cells found in the periphery. Intriguingly, when the mHEL transgene was replaced by a soluble form of HEL (sHEL), the double transgenic mice were able to generate mature B cells in the periphery. However, while these

## Significance

BCR cross-linking has been shown to trigger a signal transduction cascade that involves coordinated functions of kinases, adaptor molecules, and phosphatases. The present study demonstrates that BCR signaling in immature B cells is in part regulated by a lysosomal protein, LAPTM5. Our results uncover a previously unidentified LAPTM5-WWP2-PTEN cascade that regulates immature B cell apoptosis and contributes to B cell tolerance.

Author affiliations: <sup>a</sup>Department of Immunology, School of Basic Medical Sciences, Fudan University, Shanghai 200032, China; <sup>b</sup>Department of Immunology, Medical Research Institute, Tokyo Medical and Dental University, Tokyo 113-8510, Japan; <sup>c</sup>Department of Clinical Immunology, Children's Hospital of Fudan University, National Children's Medical Center, Shanghai 201102, China; <sup>d</sup>School of Basic Medical Sciences, Fudan University, Shanghai 200032, China; <sup>e</sup>Department of Rheumatology, University of Chicago Medicine, Chicago, IL 60637; <sup>f</sup>Department of Microbiology and Immunology, College of Basic Medical Sciences, Zhengzhou University, Zhengzhou 450001, China; <sup>g</sup>Division of Biochemistry, Faculty of Pharmacy and Graduate School of Pharmaceutical Science, Keio University, Tokyo 105-8512, Japan; and <sup>h</sup>Shanghai Huashen Institute of Microbes and Infections, Shanghai 200030, China

Author contributions: Y.W. and J.L. performed most of the experiments; Y.W., H. Zhu, K.L., and H.-Y.Z. conducted immunoblot and immunofluorescence staining and prepared cells for 4D label-free proteomic analysis; J.L., R.Z., and H. Zhang performed animal experiments and measured serum autoantibodies levels; C.A., T.T., and M.G.W. established *Laptm5*<sup>-/-</sup>56R mice; Q.M., X.M., and C.C. analyzed and interpreted data; Y.T., M.Y., Y.L., X.F., H.W., Z.W., and S.J. interpreted data and supervised the study; and Y.W., J.L., and J.-Y.W. prepared figures and wrote the paper.

The authors declare no competing interest.

This article is a PNAS Direct Submission.

Copyright © 2022 the Author(s). Published by PNAS. This article is distributed under [Creative Commons Attribution-NonCommercial-NoDerivatives License 4.0 \(CC BY-NC-ND\)](https://creativecommons.org/licenses/by-nc-nd/4.0/).

<sup>1</sup>Y.W. and J.L. contributed equally to this work.

<sup>2</sup>To whom correspondence may be addressed. Email: wang@fudan.edu.cn.

This article contains supporting information online at <http://www.pnas.org/lookup/suppl/doi:10.1073/pnas.2205629119/-DCSupplemental>.

Published August 29, 2022.

B cells expressed anti-HEL BCR, they were in an anergic status and functionally nonresponsive to the antigen stimulation (18).

The 56R HC knockin mice represent a unique model to study B cell tolerance (19). The 56R HC binds DNA with high avidity when paired with most of the endogenous light chains. Only a few light chains, called editors, are able to inhibit/reduce DNA binding and allow the survival and maturation of immature B cells. It was found that Vk21D abrogated DNA binding, whereas Vk38C allowed DNA binding with low avidity. Therefore, 56R knockin mice are suitable for studying the generation and fate of both high- and low-avidity autoreactive B cells in the same *in vivo* system (19–21).

Lysosomal-associated protein transmembrane 5 (LAPTM5) is a 30-kDa protein expressed in lymphoid and myeloid cells (22). It contains five transmembrane domains, three multipolyproline tyrosine (PY) motifs, and one ubiquitin interaction motif (UIM) (22, 23). LAPTM5 has been shown to interact with HECT-type ubiquitin ligase family members, including NEDD4 (neural precursor cell expressed developmentally down-regulated protein 4) and ITCH (24, 25). LAPTM5-NEDD4 interaction, mediated by the PY motifs of LAPTM5 and NEDD4-WW domains, are essential for the lysosomal sorting of LAPTM5 (25). Our previous studies revealed that LAPTM5 suppresses excessive T cell activation by down-modulating surface T cell receptor (TCR) levels (26). In addition, we have shown that LAPTM5 negatively regulates surface BCR levels on mature B cells and that LAPTM5 deficiency results in enhanced B cell activation and autoantibody production (27). LAPTM5 also mediates the down-modulation of the pre-BCR in early B lineage cells and positively regulates inflammatory signaling pathways in macrophages (28, 29). These observations suggest that LAPTM5 may be involved in the regulation of multiple pathways in immune cells.

In the present study, we have explored the role of LAPTM5 in B cell tolerance. We used 56R HC knockin mice to elucidate the contribution of LAPTM5 in the elimination and selection of high and low avidity autoreactive B cells. We also used a model immature B cell line, WEHI231, to delineate the molecular mechanism of LAPTM5-mediated apoptosis. We showed that LAPTM5 was involved in the elimination of autoreactive immature B cells in the BM and also limited the ability of low-avidity autoreactive B cells to become marginal zone B (MZB) cells. Detailed molecular and proteomics analyses revealed that LAPTM5 targets the E3 ubiquitin ligase WW domain-containing protein 2 (WWP2) for lysosomal degradation, resulting in the accumulation of its substrate PTEN and decreased AKT phosphorylation. Our results reveal a previously unidentified mechanism that contributes to immature B cell apoptosis and B cell tolerance.

## Results

**Increased Immature B Cell Population in *Laptm5*<sup>-/-</sup> 56R Mice Relative to 56R Mice.** To investigate whether and how LAPTM5 might be involved in eliminating autoreactive immature B cells *in vivo*, we bred *Laptm5*<sup>-/-</sup> mice with anti-DNA heavy chain (56R) knockin mice, a model for studying B cell tolerance (19, 21). We first compared early B cell development in wild-type (WT), 56R, *Laptm5*<sup>-/-</sup>, and *Laptm5*<sup>-/-</sup> 56R mice. While the total cellularity in the BM was similar among these mice, the number of spleen cells was decreased in mice with the 56R background (*SI Appendix, Table S1*). B220<sup>+</sup> cells were decreased in spleen of 56R mice and *Laptm5*<sup>-/-</sup> 56R mice compared with WT and *Laptm5*<sup>-/-</sup> mice (*SI Appendix, Table S1*). Flow cytometric analysis of BM cells revealed that the percentages and

numbers of recirculating B cells (B220<sup>hi</sup>CD43<sup>-</sup>) were decreased in mice on the 56R background (Fig. 1 *A, Upper*, and B and *SI Appendix, Table S2*). Among the B220<sup>+</sup>CD43<sup>-</sup> cells, the proportion of pre-B cells was increased in 56R and *Laptm5*<sup>-/-</sup> 56R mice (Fig. 1 *A, Lower*). In agreement with previous findings, the proportion and numbers of immature B cells were dramatically decreased in 56R mice compared with WT mice (Fig. 1 *A, Lower*, and C and *SI Appendix, Table S2*) because most of the immature B cells bearing 56R HC are autoreactive and thus eliminated. Remarkably, the immature B population was significantly increased in *Laptm5*<sup>-/-</sup> 56R mice compared with 56R mice (Fig. 1 *A, Lower*, and C and *SI Appendix, Table S2*), suggesting that LAPTM5 deficiency allowed the survival of some autoreactive immature B cells that were otherwise deleted by apoptosis. Indeed, immature B cells from *Laptm5*<sup>-/-</sup> 56R mice contained a significantly lower proportion of 7-AAD<sup>+</sup> dead cells than those from 56R mice (Fig. 1*D*).

To further reveal the role of LAPTM5 in B cell development in the BM, we performed single-cell RNA sequencing (scRNA-Seq) of BM B220<sup>+</sup> cells from 56R and *Laptm5*<sup>-/-</sup> 56R mice. The dataset contained 6,951 single B cells (2,961 cells from 56R and 3,990 cells from *Laptm5*<sup>-/-</sup> 56R mice). These cells were classified into 11 unique clusters by unsupervised hierarchical clustering and visualization with uniform manifold approximation and projection (UMAP) (Fig. 1*E* and *SI Appendix, Fig. S1*). Cells in cluster 6 resembled pre/pro-B cells since they expressed genes associated with myeloid lineages such as *Runx2* (30). Cluster 9 cells were highly enriched for *Dntt*, *Ifitm2*, and *Ifitm3*, indicative of a pro-B cell phenotype. Cells in cluster 8 resembled pre-BCR<sup>+</sup> cells, as they highly expressed surrogate light chain genes, including *Vpreb1*, *Vpreb2*, and *Igll1* ( $\lambda 5$ ). Cells in clusters 4 and 5 characterized by expression of *Il7r*, *Hist1h2ap*, and *Mki67* were identified as pre-B cells. *Rag1* was highly expressed in clusters 2 and 1, which were identified as pre-B cells undergoing  $\kappa$ - and  $\lambda$ -gene rearrangement, respectively, based on their expression of *Igkc* and *Iglc*. Cells in cluster 0 were immature B since they expressed *Mas4a1* and *fcmr* but did not express *Rag1*. Cells in cluster 3 were enriched for *H2-Aa*, *Fcer2a*, and *cd55*, indicative of a mature B cell phenotype. Cells of an activated phenotype (cluster 7) were also observed, characterized by the expression of *cd83* (31). Cluster 10 expressed *Igha*, *mzb1*, and *Jchain* and were plasma cells (*SI Appendix, Figs. S1 A and B*).

Consistent with the fluorescence-activated cell sorting (FACS) data, *Laptm5*<sup>-/-</sup> 56R mice contained increased proportions of immature B and mature B cells compared to 56R mice (Fig. 1 *E* and *F*). In addition, quantitative set analysis for gene expression (QuSAGE) analysis revealed that immature B cells from *Laptm5*<sup>-/-</sup> 56R mice were enriched in PI3K-Akt, mTOR, Ras, and MAPK signaling pathways that contribute to cell survival (Fig. 2*A*), in agreement with the decreased death in these cells as compared with immature B cells from 56R mice (Fig. 1*D*). Moreover, mature B cells from *Laptm5*<sup>-/-</sup> 56R mice were enriched for activated autoimmune disease and transplant rejection pathways compared with those from 56R mice, suggesting that *Laptm5*<sup>-/-</sup> 56R mice may be more susceptible to autoimmunity (Fig. 2*A* and *SI Appendix, Fig. S2*). We next performed single-cell BCR sequencing (scBCR-Seq) of these cells. Although 56R mice were heterozygous for the 56R allele, most B cells used 56R heavy chain (IGHV1-82) and *Laptm5*<sup>-/-</sup> 56R mice had higher usage of IGHV1-82 than did 56R mice (*SI Appendix, Fig. S3 A, Upper*). Light chain usage was similar between 56R and *Laptm5*<sup>-/-</sup> 56R mice, and IGKV19-93 (Vk38C) was most commonly used (*SI Appendix, Fig. S3 A,*

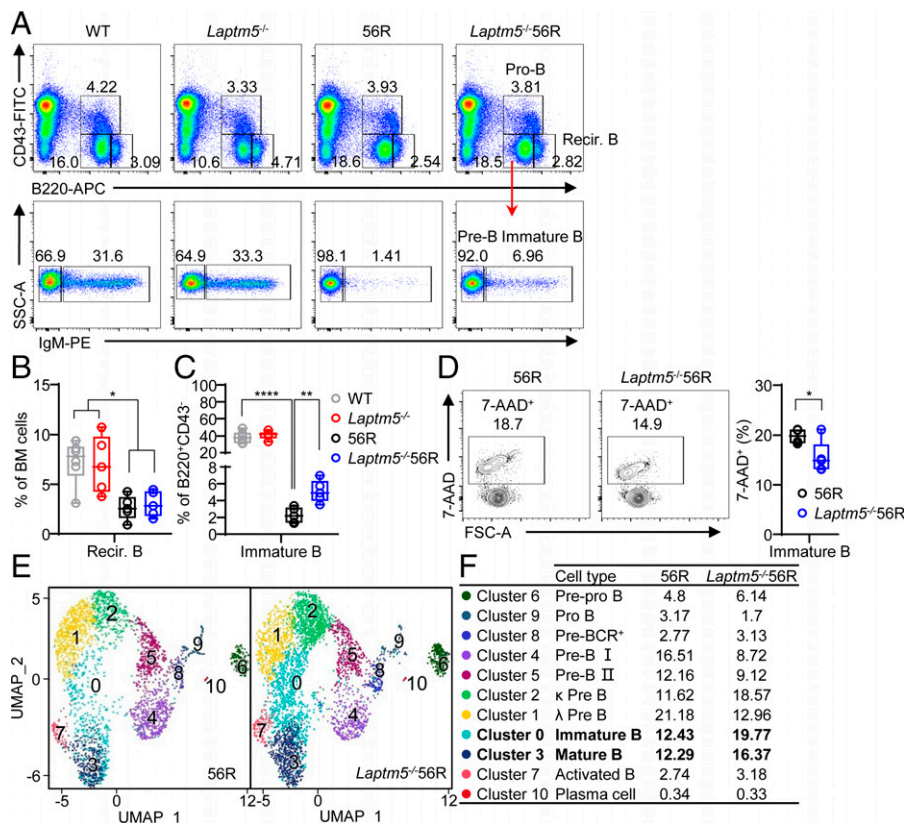


**Fig. 1.** Increased immature B cell population in the BM of *Laptm5*<sup>-/-</sup>56R mice compared with 56R mice. (A) Representative FACS profiles showing the pro-B (B220<sup>+</sup>CD43<sup>+</sup>) and recirculating B cells (B220<sup>hi</sup>CD43<sup>-</sup>) (Upper), and pre-B (B220<sup>+</sup>CD43<sup>-</sup>IgM<sup>-</sup>) and immature B (B220<sup>+</sup>CD43<sup>-</sup>IgM<sup>+</sup>) (Lower) populations in the BM. (B and C) Percentages of recirculating (B) and immature (C) B cells in WT, *Laptm5*<sup>-/-</sup>, 56R, and *Laptm5*<sup>-/-</sup>56R mice (*n* = 5 or 6). (D) Increased proportion of 7-AAD<sup>+</sup> dead immature B cells in *Laptm5*<sup>-/-</sup>56R relative to 56R mice. Left, representative FACS profiles; Right, percentages of 7-AAD<sup>+</sup> cells in gated immature B cells from 7-wk-old age-matched 56R and *Laptm5*<sup>-/-</sup>56R mice (*n* = 5). (E) UMAP projection of BM B220<sup>+</sup> cells with major subsets color coded by assigned cell type showing 2,961 cells from three 56R mice (Left) and 3,990 cells from three *Laptm5*<sup>-/-</sup>56R mice (Right). (F) Frequency of all cell types in 56R and *Laptm5*<sup>-/-</sup>56R mice. \**P* < 0.05; \*\**P* < 0.01; \*\*\*\**P* < 0.0001.

Middle and Bottom). In 56R mice, immature B cells that bind DNA with low affinity, including those expressing Vκ38C, were allowed to survive (19–21). *Laptm5*<sup>-/-</sup>56R mice had an increased immature B population compared with 56R mice (Fig. 1 A, Lower and SI Appendix, Table S2), suggesting that more low-affinity immature B cells survived in the absence of LAPT5. The similar LC usage between 56R and *Laptm5*<sup>-/-</sup>56R mice suggests that Vκ38C<sup>+</sup> and other Vκ<sup>+</sup> immature B cells were all increased in *Laptm5*<sup>-/-</sup>56R mice as compared with 56R mice. We further compared the LC repertoire between immature and mature B cells expressing 56R HC. In 56R mice, among the 72 LC sequences derived from immature B cells, 32 distinct sequences were found (44.4%) (Fig. 2 B, Upper Left). In contrast, 94 LC sequences from mature B cells contained only 20 unique sequences (21.3%) (Fig. 2 B, Upper Right), representing 52% reduction in the LC diversity in mature B compared with immature B cells in 56R mice. In *Laptm5*<sup>-/-</sup>56R mice, 89 of 285 LC sequences in immature B cells were unique (Fig. 2 B, Lower Left) while 43 of 241 LC sequences in mature B cells were unique (Fig. 2 B, Lower Right), equivalent to 43% reduction in LC diversity in mature B cells. Therefore, LAPT5 deficiency reduced the extent to which LC diversity was reduced between immature and mature B cell stages.

**Increased Vκ38C<sup>+</sup> MZB Cells in *Laptm5*<sup>-/-</sup>56R Mice.** Consistent with the reduction of immature B cells in the BM of 56R and *Laptm5*<sup>-/-</sup>56R mice, the percentages and numbers of transitional B (B220<sup>+</sup>AA4.1<sup>+</sup>) and mature B cells (B220<sup>+</sup>AA4.1<sup>-</sup>) were both decreased in these mice compared with WT and

*Laptm5*<sup>-/-</sup> mice (SI Appendix, Fig. S4 A, B, and F). Among the transitional B cells, the distribution of T1, T2, and T3 subpopulations was quite similar (SI Appendix, Fig. S4 C–E). Within the mature B cells, the proportion of marginal zone B (MZB, CD21<sup>high</sup>CD23<sup>low</sup>) cells was significantly increased while that of follicular B (FOB, CD23<sup>high</sup>CD21<sup>low</sup>) cells was decreased in 56R and *Laptm5*<sup>-/-</sup>56R mice compared with WT and *Laptm5*<sup>-/-</sup> mice (SI Appendix, Fig. S5 A, Upper, B, and C), in agreement with earlier observations in 56R mice (21).

We next analyzed whether LAPT5 deficiency affected the maturation of 56R B cells expressing Vκ38C or Vκ21D editor light chains. Remarkably, *Laptm5*<sup>-/-</sup>56R mice contained a significantly higher percentage of Vκ38C<sup>+</sup> MZBs with a concomitant decrease of Vκ21D<sup>+</sup> MZB cells compared with 56R mice (Fig. 2 C and D). In contrast, FOB cells from *Laptm5*<sup>-/-</sup>56R and 56R mice contained similar proportion and numbers of Vκ38C<sup>+</sup> and Vκ21D<sup>+</sup> cells (SI Appendix, Fig. S5 D and E). Taken together, the above results indicate that LAPT5 deficiency allows more Vκ38C<sup>+</sup> autoreactive B cells to become MZB cells.

**LAPT5 Deficiency Results in Increased Autoantibody Production.** The 56R HC recognizes DNA with low avidity when paired with the Vκ38C light chain. The increased Vκ38C<sup>+</sup> MZB cells in *Laptm5*<sup>-/-</sup>56R mice may result in increased production of anti-DNA autoantibodies. MZB cells are known to respond to blood-borne antigens and rapidly differentiate into IgM-secreting plasma cells (4, 32–34). Indeed, we found that *Laptm5*<sup>-/-</sup>56R mice produced higher levels of IgM



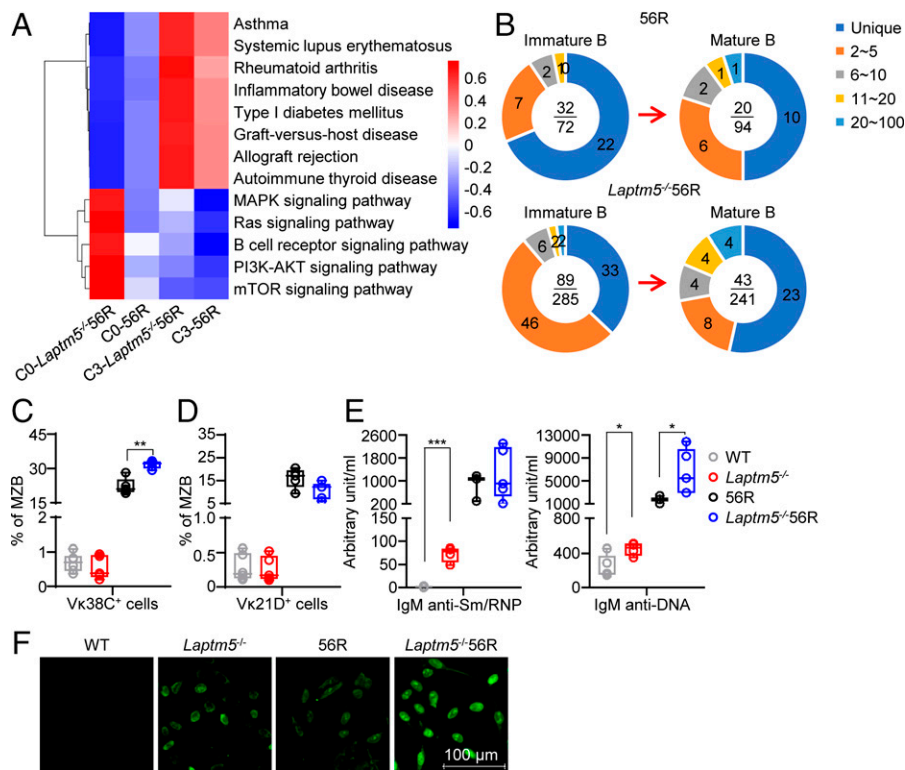


**Fig. 2.** Increased autoreactive B cells and elevated autoantibody levels in *Laptm5*<sup>-/-</sup>56R compared with 56R mice. (A) Heatmap of differentially activated pathways in the immature and mature B cells from 56R and *Laptm5*<sup>-/-</sup>56R mice. C0, immature B; C3, mature B cells. (B) Pie chart representations of clone distribution of immature B and mature B cells expressing 56R heavy chain from 56R (Upper) and *Laptm5*<sup>-/-</sup>56R (Lower) mice. Numbers above and below the line in the center of the pie chart indicate unique and total sequences, respectively. (C and D) Percentages of Vκ38C<sup>+</sup> (C) and Vκ21D<sup>+</sup> (D) cells in the gated MZB population. (E) Left, elevated levels of IgM anti-Sm/RNP antibodies in *Laptm5*<sup>-/-</sup> relative to WT mice; Right, *Laptm5*<sup>-/-</sup> and *Laptm5*<sup>-/-</sup>56R mice produced elevated levels of IgM anti-DNA antibodies compared to WT and 56R mice, respectively. The 70-wk-old age-matched WT, *Laptm5*<sup>-/-</sup>, 56R, and *Laptm5*<sup>-/-</sup>56R mice (*n* = 3 or 5) were bled, and serum levels of IgM anti-Sm/RNP and IgM anti-DNA were measured by enzyme-linked immunosorbent assay (ELISA). (F) Serum levels of IgM anti-nuclear antibodies were detected by HEP2 reactivity. Each symbol in C and D represents an individual mouse and means ± SD are shown. \**P* < 0.05; \*\**P* < 0.01; \*\*\**P* < 0.001.

anti-DNA and IgM anti-nuclear antibodies than 56R mice (Fig. 2 E, Right, and F and SI Appendix, Fig. S6B). In addition, *Laptm5*<sup>-/-</sup> mice produced elevated levels of both anti-Sm/RNP and anti-DNA autoantibodies than WT mice (Fig. 2 E, Left), which was in agreement with our previous study (27). Total serum IgM levels were not significantly different among these mice (SI Appendix, Fig. S6A). Serum concentrations of IgG anti-DNA and anti-Sm/RNP autoantibodies were not different between 56R and *Laptm5*<sup>-/-</sup>56R mice (SI Appendix, Fig. S6 C and D). These results suggest an important function for LAPT5 in limiting autoreactive B cells to become MZB cells and secrete autoreactive IgM antibodies.

**BCR Cross-Linking Induces Immature B Cell Apoptosis in Part through Up-Regulation of LAPT5.** Earlier studies have shown that immature B cells in the BM are susceptible to tolerance and undergo apoptosis upon BCR cross-linking (35, 36). To examine whether LAPT5 is involved in B cell tolerance, we cultured BM cells in the presence of different concentrations of anti-IgM antibody (α-IgM), and analyzed cell death in gated immature B populations by flow cytometry. As shown in Fig. 3A, LAPT5-deficient immature B cells showed reduced cell death compared with WT immature B cells, suggesting that LAPT5 deficiency rendered immature B cells more resistant to death induced by BCR stimulation.

To elucidate the molecular mechanism by which LAPT5 promotes immature B cell apoptosis and contributes to B cell tolerance, we then used a model B cell line, WEHI231. Like BM immature B cells, WEHI231 cells undergo apoptosis upon

BCR stimulation. We found that α-IgM treatment up-regulated LAPT5 protein expression in WEHI231 cells (Fig. 3B) and subsequently triggered their death (Fig. 3C). Cell cycle analysis revealed that α-IgM-induced cell cycle arrest at the G<sub>1</sub> phase in WEHI231 cells before induction of apoptosis (SI Appendix, Fig. S7A). To examine whether the up-regulation of LAPT5 is involved in apoptosis, we established LAPT5-deficient WEHI231 cells by CRISPR-CAS9-mediated genome editing (SI Appendix, Fig. S7B). We found that all three LAPT5-deficient clones (A2, A4, and A6) showed significantly reduced apoptosis compared with WT WEHI231 cells (Fig. 3D), indicating that α-IgM-induced apoptosis was in part mediated by LAPT5.

BCR cross-linking leads to phosphorylation of immunoreceptor tyrosine-based activation motifs (ITAMs), and activated ITAMs recruit SYK, which propagates the activation signal to downstream crucial signaling intermediates, such as AKT (32, 33, 37). In WEHI231 cells, interestingly, phosphorylation of SYK, ERK, and AKT was sharply reduced at 24 and 48 h after BCR engagement (Fig. 3E and SI Appendix, Fig. S7C). It has been shown that reduction in p-AKT levels leads to accumulation of FOXO1 and the expression of its target genes, including the cell cycle inhibitor CDKN1B (p27Kip1) and the proapoptotic BH3-only protein BCL2L11 (BIM) (34). Indeed, both p27Kip1 and BIM were up-regulated in α-IgM-stimulated WEHI231 cells (Fig. 3E and SI Appendix, Fig. S7C). Intriguingly, the p27Kip1 protein level was elevated from 24 h, whereas the BIM level was higher at 48 h than 24 h after α-IgM stimulation, which is consistent with the cell cycle arrest

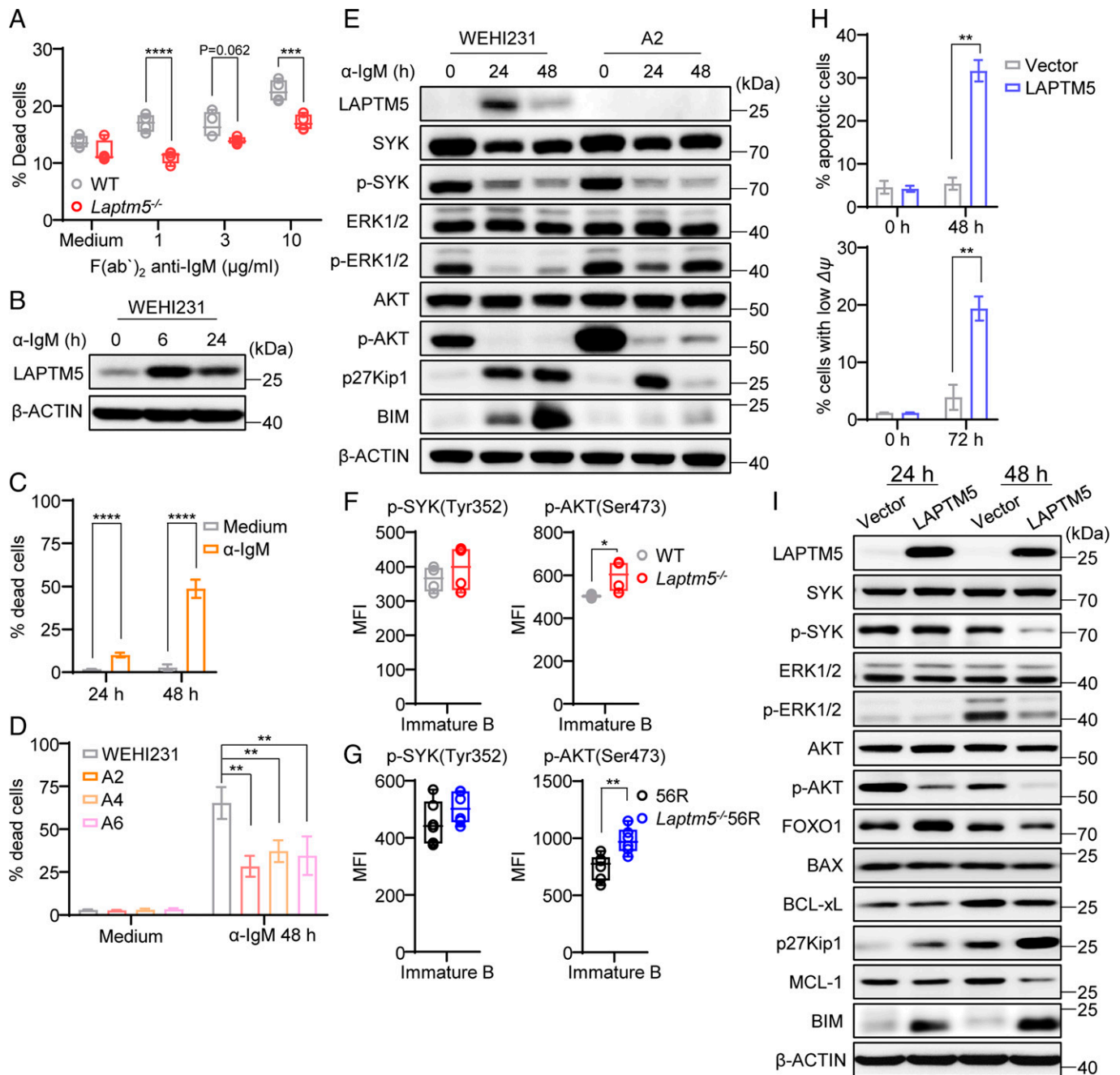


**Fig. 3.** Anti-IgM-induced immature B cell death is in part mediated by LAPTMS. (A) LAPTMS-deficient immature B cells were more resistant to  $\alpha$ -IgM-induced death. BM cells isolated from 7-wk-old WT and LAPTMS-deficient mice ( $n = 4$ ) were cultured in the presence of different concentrations of  $\alpha$ -IgM antibodies for 6 h and analyzed for the proportion of 7-AAD<sup>+</sup> cells by FACS in gated immature B cells (B220<sup>dull</sup>IgD<sup>-</sup>Ig $\kappa$ <sup>+</sup>). (B) LAPTMS protein expression was up-regulated in WEHI231 cells by  $\alpha$ -IgM stimulation (10  $\mu$ g/mL). (C) BCR cross-linking induced death of WEHI231 cells. WEHI231 cells were cultured in the presence of 10  $\mu$ g/mL  $\alpha$ -IgM and analyzed for cell viability 24 and 48 h after the culture. (D) Reduced apoptosis in LAPTMS-deficient WEHI231 cells (clones A2, A4, and A6) after  $\alpha$ -IgM stimulation. Mean  $\pm$  SD of five experiments is shown. (E) Analysis of BCR signaling events in WEHI231 and A2 cells before and after  $\alpha$ -IgM (10  $\mu$ g/mL) stimulation for 24 and 48 h. (F and G) Mean fluorescence intensity (MFI) of p-SYK (Left) and p-AKT (Right) in immature B cells of WT and *Laptm5*<sup>-/-</sup> ( $F, n = 4$ ) or 56R and *Laptm5*<sup>-/-</sup> 56R mice ( $G, n = 6$ ). (H) Ectopic expression of LAPTMS induced apoptosis of WEHI231 cells. WEHI231 cells were transduced with retrovirus expressing LAPTMS-IRES-GFP or GFP alone (vector) and analyzed for annexin V<sup>+</sup> cells at 48 h (Upper) and mitochondrial membrane potential at 72 h (Bottom) in the gated GFP<sup>+</sup> population. A summary of three independent experiments is shown. (I) Immunoblot of molecules involved in BCR signaling and apoptosis after ectopic expression of LAPTMS in WEHI231 cells. \* $P < 0.05$ ; \*\* $P < 0.01$ ; \*\*\* $P < 0.005$ ; \*\*\*\* $P < 0.0001$ .

observed at 24 h (SI Appendix, Fig. S7A) followed by apoptosis at 48 h after stimulation (Fig. 3C). Similar to WEHI231 cells, LAPTMS-deficient WEHI231 cells (A2) also down-regulated p-SYK levels (Fig. 3E). However, A2 cells had higher levels of p-ERK and p-AKT than did WEHI231 cells before and after  $\alpha$ -IgM stimulation and only moderately up-regulated p27Kip1 and BIM protein expression at 48 h after  $\alpha$ -IgM stimulation

(Fig. 3E and SI Appendix, Fig. S7C). In agreement with the findings in WEHI231 and A2 cells, LAPTMS-deficient BM immature B cells showed similar levels of p-SYK but higher levels of p-AKT than did WT BM immature B cells (Fig. 3F and SI Appendix, Fig. S7D). Moreover, *Laptm5*<sup>-/-</sup> 56R immature B cells showed similar levels of p-SYK but higher levels of p-AKT compared with 56R immature B cells (Fig. 3G and SI

*Appendix, Fig. S7E*). Therefore, LAPT<sub>M5</sub> negatively regulated p-AKT levels both in WEHI231 and BM immature B cells.

**Ectopic Expression of LAPT<sub>M5</sub> Triggers Apoptosis of WEHI231 Immature B Cells.** Having shown that LAPT<sub>M5</sub> contributed to  $\alpha$ -IgM-induced apoptosis of WEHI231 cells, we then investigated whether ectopic LAPT<sub>M5</sub> expression, in the absence of BCR cross-linking, could mimic  $\alpha$ -IgM stimulation and induce cell cycle arrest and apoptosis in these cells. In agreement with our previous results (27), ectopic LAPT<sub>M5</sub> expression dose-dependently down-modulated BCR levels in WEHI231 cells (*SI Appendix, Fig. S8 A and B*). In addition, LAPT<sub>M5</sub>-expressing GFP<sup>+</sup> cells were counterselected during culture, as indicated by the gradual decline of the GFP<sup>+</sup> population and rapid loss of the GFP<sup>high</sup> cells (*SI Appendix, Fig. S8 C, Left and Middle*) compared with cells expressing vector (GFP) alone. Consequently, LAPT<sub>M5</sub>-transduced cells showed decreased proliferation relative to cells expressing vector alone (*SI Appendix, Fig. S8 C, Right*). Cell cycle analysis revealed that ectopic expression of LAPT<sub>M5</sub> induced G<sub>1</sub> arrest and led to increased percentage of sub-G<sub>1</sub> cells (*SI Appendix, Fig. S8D*). Further experiments showed that LAPT<sub>M5</sub>-induced apoptosis was accompanied by an increased percentage of cells with low mitochondrial membrane potential (Fig. 3H and *SI Appendix, Fig. S9 A and B*). Immunoblot analysis confirmed that LAPT<sub>M5</sub> induced the accumulation of apoptosis-associated proteins, activated caspase 3 and cleaved PARP, but did not up-regulate molecules related to pyroptosis (caspase 11) (*SI Appendix, Fig. S9C*). At 48 h after ectopic LAPT<sub>M5</sub> expression, there was a moderate decrease in the microtubule-associated light chain 3B-1 (LC3B-1) and an increase in the autophagosome-associated LC3B-II expression, suggesting that LAPT<sub>M5</sub>-induced apoptosis in WEHI231 cells may be accompanied by autophagy. These observations demonstrate that, instead of BCR cross-linking, ectopic expression of LAPT<sub>M5</sub> alone could trigger cell cycle arrest and apoptosis in WEHI231 immature B cells.

Ectopic LAPT<sub>M5</sub> expression in WEHI231 cells also triggered signaling events similar to those elicited by BCR cross-linking. p-SYK and p-ERK levels were reduced at 48 h after LAPT<sub>M5</sub> expression (Figs. 3I and *SI Appendix, Fig. S9D*). The p-AKT level was decreased, whereas the levels of p27Kip1 and BIM were both up-regulated (Fig. 3I and *SI Appendix, Fig. S9D*). The slightly delayed kinetics in the phosphorylation of signaling molecules and up-regulation of p27Kip1 could be due to the time period needed for LAPT<sub>M5</sub> expression after retrovirus transduction. Moreover, we found that FOXO1 was up-regulated at 24 h while the expression of the antiapoptotic Mcl-1 was reduced at 48 h after LAPT<sub>M5</sub> expression (Fig. 3I and *SI Appendix, Fig. S9D*). The levels of BAX and BCL-xL were not affected (Fig. 3I and *SI Appendix, Fig. S9D*). Therefore, ectopic LAPT<sub>M5</sub> expression not only induced cell cycle arrest and apoptosis in WEHI231 cells but also recapitulated signaling events triggered by BCR cross-linking. Along with the finding that  $\alpha$ -IgM stimulation up-regulated LAPT<sub>M5</sub> protein expression, our data indicate that LAPT<sub>M5</sub> is a mediator of  $\alpha$ -IgM-induced cell cycle arrest and apoptosis in WEHI231 cells.

**LAPT<sub>M5</sub> Inhibits AKT Phosphorylation by Up-Regulating PTEN Levels.** AKT phosphorylation is known to be enhanced by PI3K (phosphoinositide 3-kinase) but inhibited by PTEN (phosphatase and tensin homolog), a phosphatase that antagonizes PI3K activity (38). We found that A2 cells had lower basal levels of PTEN than WEHI231 cells (Fig. 4 A and B, 0 h).  $\alpha$ -IgM stimulation up-regulated LAPT<sub>M5</sub> protein expression in WEHI231

but not A2 cells, and again A2 cells had lower levels of PTEN compared with WEHI231 cells (Fig. 4 A and B, 24 h and 48 h). Consistently, compared with WT BM immature B cells, *Laptm5*<sup>-/-</sup> BM immature B cells expressed lower levels of PTEN before and after  $\alpha$ -IgM stimulation (Fig. 4C). Moreover, PTEN levels were also lower in *Laptm5*<sup>-/-</sup>56R immature B than 56R immature B cells (Fig. 4D). These observations suggested that  $\alpha$ -IgM stimulation may up-regulate PTEN protein levels through LAPT<sub>M5</sub>. To explore this possibility, we ectopically expressed LAPT<sub>M5</sub> in WEHI231 cells. We found that LAPT<sub>M5</sub> expression indeed led to increased PTEN level, whereas the levels of PI3K catalytic subunit P110 $\delta$  and the regulatory subunit P85, as well as mTOR and p-mTOR, remained unchanged (Fig. 4 E and F). To further validate the relationship of LAPT<sub>M5</sub> with PTEN and p-AKT, we compared PTEN and p-AKT levels in WEHI231 and A2 cells. As shown in Fig. 4 G and H, WEHI231 cells had higher levels of PTEN and lower level of p-AKT than A2 cells (compare vector lanes of WEHI231 and A2 in Fig. 4G), suggesting that the endogenous LAPT<sub>M5</sub> caused an increased level of PTEN and a decreased level of p-AKT. Moreover, ectopic expression of LAPT<sub>M5</sub> resulted in higher PTEN and lower p-AKT levels both in WEHI231 and A2 cells (Fig. 4 G and H). These results suggest that LAPT<sub>M5</sub> up-regulates PTEN levels, thereby upsetting the balance between PI3K and PTEN activities, resulting in the inhibition of AKT phosphorylation.

PTEN functions as a tumor suppressor by negatively regulating the AKT/PKB signaling pathway (39, 40). PTEN can be regulated at both transcriptional and posttranscriptional levels (41). As shown in Fig. 4I, the levels of PTEN transcripts were not affected by increased LAPT<sub>M5</sub> expression. Using cycloheximide (CHX), which inhibits new protein synthesis, the half-life of PTEN protein was found to be 6.06 h in LAPT<sub>M5</sub>-expressing WEHI231 cells and 5.74 h in control cells (Fig. 4 J and K). However, since LAPT<sub>M5</sub> protein expression was only sustained for  $\sim$ 1 h in the presence of CHX, it was difficult to conclude from this result whether LAPT<sub>M5</sub> regulated PTEN stability.

**LAPT<sub>M5</sub> Interacts with WWP2 and Promotes WWP2 Degradation in the Lysosome.** To elucidate how LAPT<sub>M5</sub> regulated the PTEN protein level, we performed liquid chromatography mass spectrometer/mass spectrometer (LC-MS/MS) and quantification by four-dimensional (4D) label-free proteomics of proteins extracted from WEHI231 cells overexpressing LAPT<sub>M5</sub> or vector (GFP) as a control. A total of 1,234,236 spectra were detected, of which 469,610 matched with the Swissprot database (*SI Appendix, Fig. S10A*). Based on these raw data, 64,940 unique peptides and 1,607 other peptides were identified, and 6,362 proteins were finally quantified. Among them, 189 proteins that exhibited significantly differential expression levels (fold change  $>1.5$ ,  $P < 0.05$ ) between LAPT<sub>M5</sub> and control were chosen for further analysis (105 up-regulated and 84 down-regulated proteins) (*SI Appendix, Fig. S10B*). Kyoto Encyclopedia of Genes and Genomes (KEGG) pathway enrichment analysis revealed that proteins affected by LAPT<sub>M5</sub> expression presented signatures related to cell growth and death, protein folding, sorting and degradation, as well as signal transduction (*SI Appendix, Fig. S10C*). A heatmap of the LAPT<sub>M5</sub> group and vector group showed that the 189 proteins formed clearly different clusters, and three replicates of each group showed low interreplicate variation as determined by hierarchical clustering (Fig. 5A).

We did not find increased PTEN protein level by LC-MS/MS in LAPT<sub>M5</sub>-expressing WEHI231 cells. One possibility is



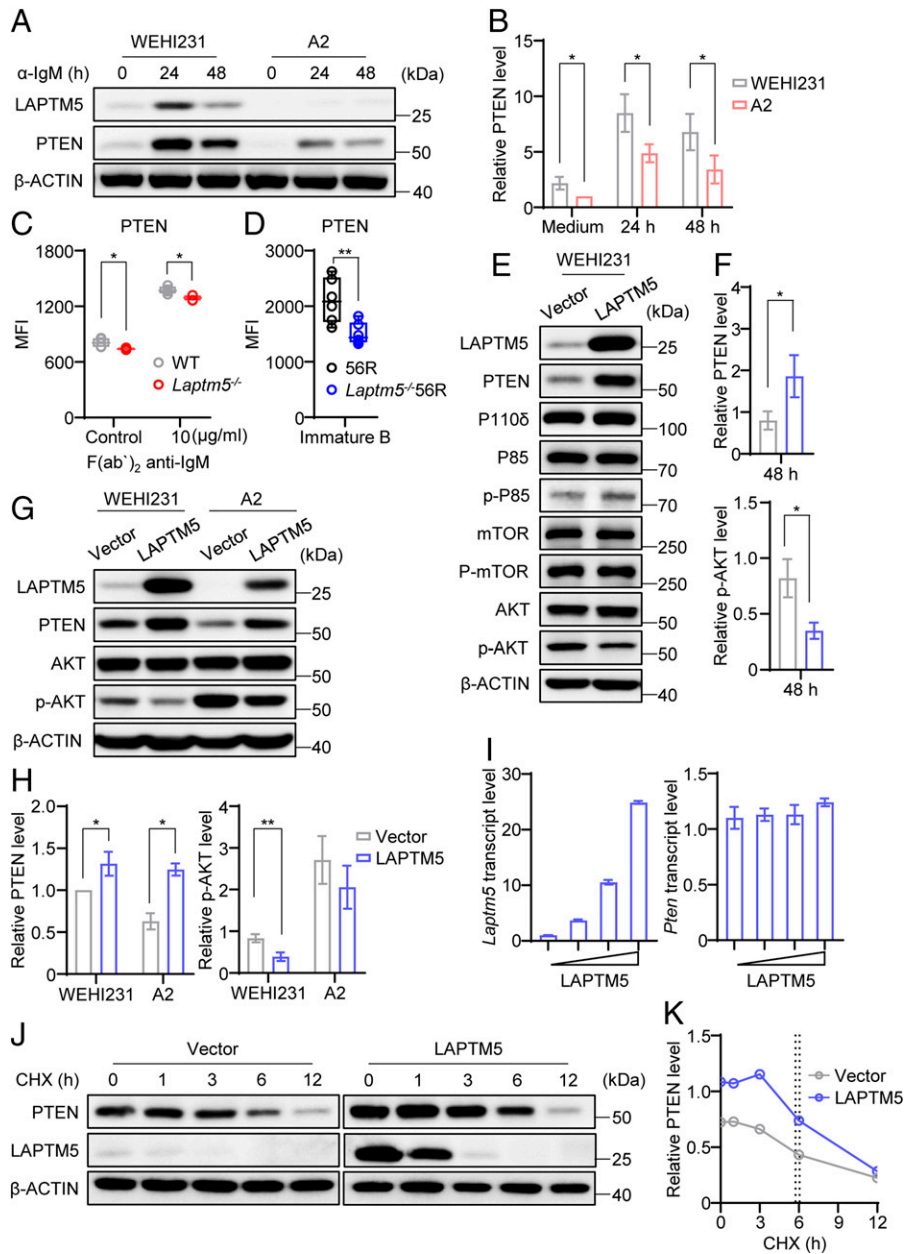


**Fig. 4.** LAPTMS enhances PTEN protein level. (A and B) PTEN protein levels in WEHI231 and A2 cells before (0 h) or after  $\alpha$ -IgM treatment for 24 and 48 h. (A) Representative results of immunoblot. (B) Summary of three independent experiments shown in A. (C) PTEN protein levels in immature B cells of WT and *Laptm5*<sup>-/-</sup> mice (*n* = 4) before and after  $\alpha$ -IgM stimulation for 6 h. (D) PTEN protein levels in immature B cells of 56R and *Laptm5*<sup>-/-</sup>56R mice (*n* = 6). (E) Immunoblot for the expression of molecules involved in the PI3K-AKT signaling pathway. (F) Quantitation of PTEN and p-AKT levels from three experiments shown in E. (G and H) LAPTMS increased PTEN and decreased p-AKT level. WEHI231 and A2 cells were transduced with retrovirus expressing empty vector or LAPTMS and analyzed for LAPTMS, PTEN, AKT, and p-AKT level by immunoblot. (H) Quantitation of PTEN (Left) and p-AKT (Right) levels from three experiments shown in G. (I) LAPTMS did not affect *Pten* transcript levels. Left, WEHI231 cells were transduced with increasing titers of retrovirus expressing LAPTMS and analyzed for the transcript levels of *Laptm5* (Left) and *Pten* (Right). (J and K) Effect of LAPTMS on PTEN protein stability. WEHI231 cells transduced with retrovirus expressing LAPTMS were treated with CHX and analyzed for PTEN and LAPTMS protein levels by immunoblot. (J) Representative blots. (K) Summary of three experiments shown in J. Each symbol in C and D represents an individual mouse and means  $\pm$  SD are shown. \**P* < 0.05; \*\**P* < 0.01.

that PTEN is rich in arginine and lysine and might have been digested into peptides that were too short to be analyzed by LC-MS/MS. Search Tool for the Retrieval of Interacting Genes (STRING) database analysis revealed that proteins interacting with PTEN included three PIK3 family members (PIK3CA/B/R1), DGL1, PTK2, TRP53, SLC9A3R1, CENPC1, NEDD4, and WWP2 (Fig. 5B). Interestingly, we found decreased WWP2 expression by LAPTMS (Fig. 5C). In agreement with the LC-MS/MS data, ectopic LAPTMS expression dose-dependently decreased WWP2 protein levels in HEK293 cells (Fig. 5D). These observations suggest that LAPTMS may target the E3 ubiquitin ligase WWP2 for degradation.

To analyze the potential interaction between LAPTMS and WWP2, we ectopically expressed LAPTMS and WWP2 in HEK293 cells and performed immunoprecipitation. As shown in Fig. 6A, LAPTMS was coprecipitated with WWP2 and conversely WWP2 could be coprecipitated by LAPTMS. We further analyzed their colocalization by confocal immunofluorescent staining and found that LAPTMS and WWP2 colocalized with LAMP1, a marker for lysosomes (Fig. 6B), suggesting that LAPTMS may promote WWP2 degradation in the lysosome. Indeed, ectopic expression of LAPTMS decreased WWP2 protein levels in HEK293 cells, and this effect could be abrogated by the addition of NH<sub>4</sub>Cl, an inhibitor of lysosome activity (Fig. 6C), but not by

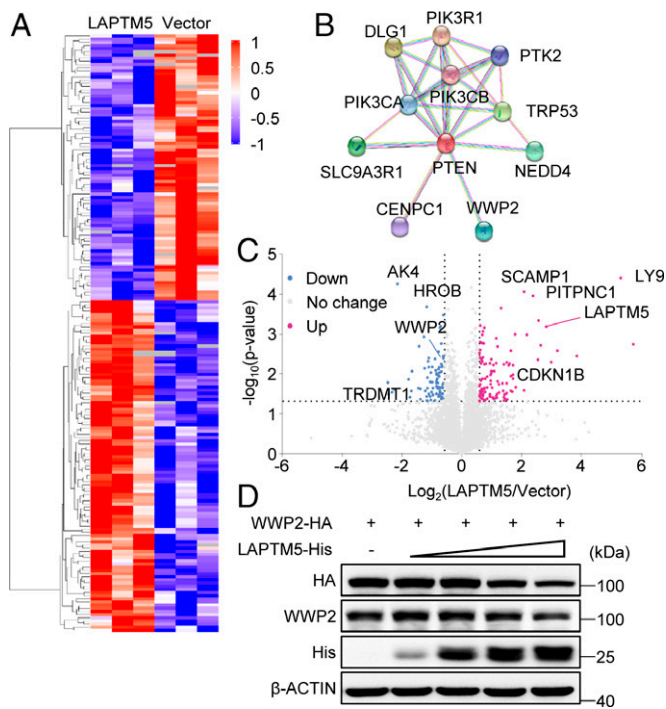


**Fig. 5.** Identification of proteins regulated by LAPTMS. WEHI231 cells were transduced with retrovirus expressing LAPTMS or vector and subjected to quantitative proteomics analysis. (A) Heatmap and clustering patterns of differentially expressed proteins in the WEHI231 cells ectopically expressing LAPTMS or vector. (B) PTEN-interacting proteins obtained from STRING online database analysis. (C) Volcano plot depicting proteins up-regulated (shown in pink) or down-regulated (blue) by ectopic LAPTMS expression compared with the control group. Significance cutoffs were set to  $P < 0.05$  and fold changes  $> 1.5$ . (D) LAPTMS promoted WWP2 degradation. HEK293 cells transfected with HA-tagged WWP2 and increasing amounts of His-tagged LAPTMS expression vector were lysed and subjected to immunoblot for HA, WWP2, His, and LAPTMS.

the proteasome inhibitor MG132 (Fig. 6D). Hence, we conclude that LAPTMS enhances PTEN protein expression by interacting with WWP2 and facilitates its lysosomal degradation.

**LAPTMS Prevented PTEN from Degradation through Its PY Motifs.** Previous studies have shown that WWP2 mediates the ubiquitination and subsequent degradation of PTEN (42, 43), suggesting the existence of the LAPTMS-WWP2-PTEN pathway. To delineate the relationship of LAPTMS, WWP2, and PTEN, we first transduced WEHI231 cells with retrovirus expressing LAPTMS or vector and analyzed PTEN protein levels in the absence or presence of MG132. Similar to the results shown in Fig. 4 A and D, ectopic LAPTMS expression increased the PTEN protein level in the absence of MG132 (Fig. 6 E, Left two lanes). PTEN level in vector-transduced cells was elevated in the presence of MG132 (compare the third lane with the first lane of Fig. 6E), indicating that PTEN normally underwent proteasomal degradation. Intriguingly, in the presence of MG132, ectopic expression of LAPTMS did not further increase the PTEN level, implying that LAPTMS suppressed the proteasomal degradation of PTEN, possibly by inhibiting its ubiquitination. Indeed, we found that WWP2-mediated ubiquitination of PTEN was reduced by LAPTMS (Fig. 7F).

PY motifs are important functional domains of LAPTMS since mutations of PY motifs abrogated its ability to down-regulate BCR and TCR levels (26, 27). LAPTMS has been shown to interact with the WW domain of NEDD4-1 through its PY motifs (25). Domain enrichment analysis of differentially expressed proteins showed that the WW domain was

associated with ectopic expression of LAPTMS in WEHI231 cells (SI Appendix, Fig. S10D). Therefore, we postulated that LAPTMS might also interact with WWP2 through its PY motifs and regulate WWP2-mediated PTEN ubiquitination. Indeed, immunoprecipitation and immunoblot analysis revealed that PTEN ubiquitination was abolished by WT LAPTMS but not by LAPTMS with all three PY motifs mutated (mPYs) (Fig. 6G). Consistently, mPYs failed to enhance PTEN protein levels (Fig. 6H). These results collectively demonstrate that LAPTMS interacts with WWP2 and promotes its lysosomal degradation, thereby suppressing WWP2-mediated ubiquitination and proteasomal degradation of PTEN.

## Discussion

The mechanism of B cell tolerance has been studied extensively using several mouse models. It is now clear that B cell central tolerance can be mediated by clonal deletion, receptor editing, and anergy. However, mechanisms whereby BCR cross-linking leads to apoptosis in immature B cells and the molecules involved in this process remain incompletely understood. In the present study, we provide immunological and biochemical evidence that LAPTMS is a physiological mediator of immature B cell apoptosis and that its absence exacerbated autoantibody production in 56R knockin mice. We also uncovered a LAPTMS-WWP2-PTEN molecular cascade that regulates apoptosis.

The HEL system has been widely used to investigate both clonal deletion and anergy by using transgenic mice expressing mHEL and soluble HEL, respectively (18, 44, 45). In contrast to the HEL system, B cells in 56R mice react with self-antigen (DNA). We think that the results obtained with 56R mice may represent one aspect of B cell tolerance. The 56R HC bound DNA with high avidity when paired with most of the endogenous LC, and only a few editor light chains, including Vκ21D and Vκ38C, were able to abrogate the strong autoreactivity. Consequently, the vast majority of the immature B cells in the BM were deleted in 56R mice. *Lap<sup>tm5</sup><sup>-/-</sup>* 56R mice had a moderately increased immature B population compared with 56R mice, suggesting that absence of LAPTMS allowed some of the autoreactive immature B cells to survive. However, when compared with WT or *Lap<sup>tm5</sup><sup>-/-</sup>* mice, the majority of the immature B cells were still deleted in *Lap<sup>tm5</sup><sup>-/-</sup>* 56R mice and only a fraction of the autoreactive immature B cells, which bind DNA with low affinity, were rescued by LAPTMS deficiency. It has been shown that loss of BIM inhibited immature B cell apoptosis and elimination of autoreactive B cells (46). The effect of LAPTMS deficiency on B cell tolerance resembles that observed in BIM-deficient mice (46) in that only a portion of the autoreactive B cells in the BM and spleen are rescued. In addition, similar to BIM deficiency, LAPTMS deficiency only partially inhibited α-IgM-induced apoptosis of immature B cells. Along with the finding that ectopic LAPTMS expression up-regulated BIM protein expression in WEHI231 immature B cells, these observations collectively suggest that LAPTMS contributes to B cell tolerance by up-regulating BIM.

MZBs are enriched for autoreactive specificities (47, 48). Vκ38C LC allowed DNA binding with weak avidity and indeed was enriched in the MZB compartment both in 56R and *Lap<sup>tm5</sup><sup>-/-</sup>* 56R mice. Intriguingly, we found an increased frequency of Vκ38C<sup>+</sup> MZB and a concomitant decreased frequency of the Vκ21D<sup>+</sup> cells in *Lap<sup>tm5</sup><sup>-/-</sup>* 56R mice relative to 56R mice, suggesting that LAPTMS deficiency allowed more Vκ38C<sup>+</sup> cells to survive and develop into MZB cells. Alternatively, Vκ38C<sup>+</sup> B cells in *Lap<sup>tm5</sup><sup>-/-</sup>* 56R mice were allowed to



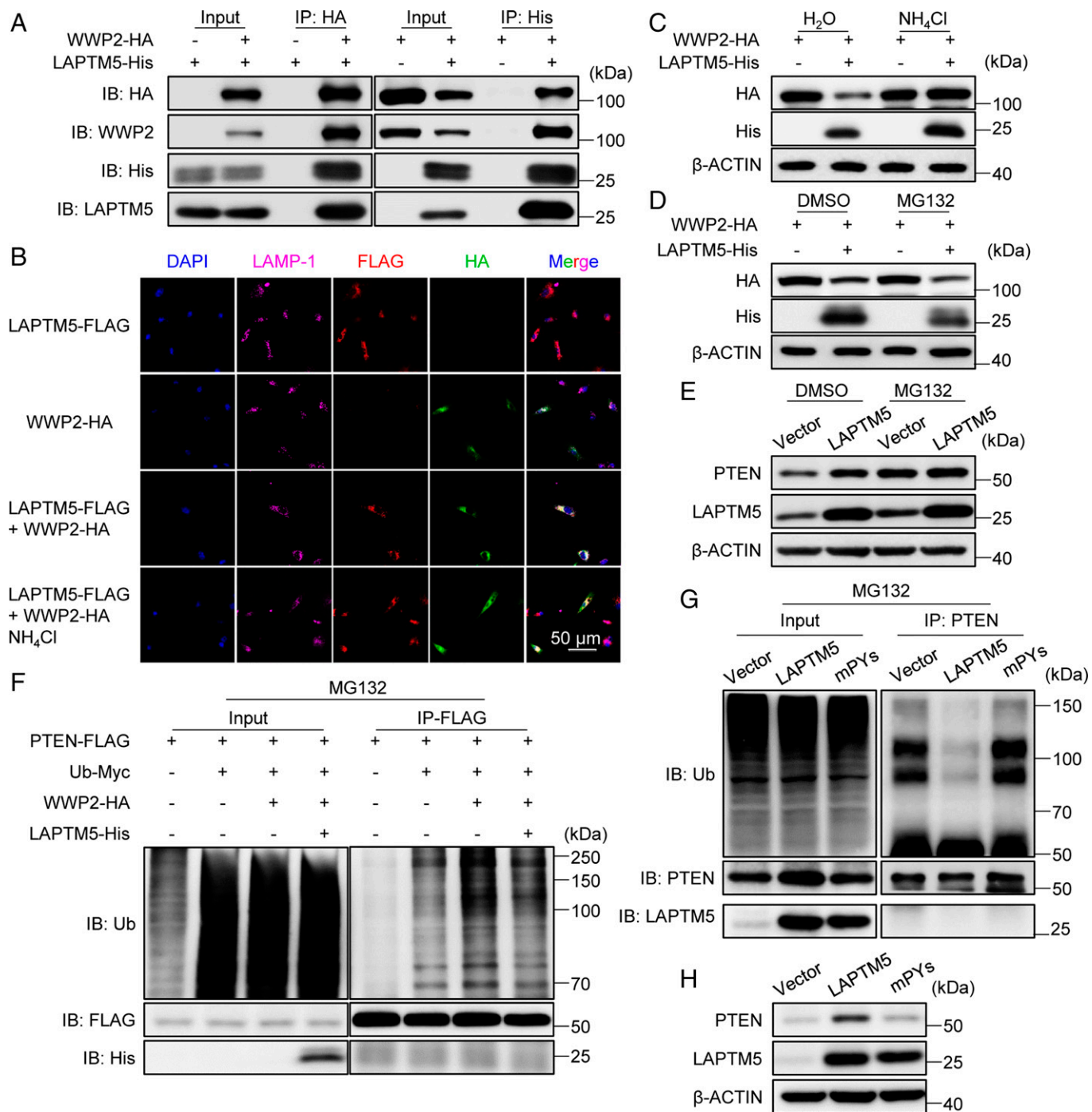


**Fig. 6.** LAPTMs interact with WWP2 and promotes its lysosomal degradation, leading to increased levels of PTEN through the PY motifs. (A) LAPTMs physically interacted with WWP2. HEK293 cells transfected with HA-tagged WWP2 and/or His-tagged LAPTMs were lysed and subjected to immunoprecipitation with  $\alpha$ -HA Ab (Left) or  $\alpha$ -His Ab (Right). Whole-cell lysate was used as input. (B) Colocalization of LAPTMs and WWP2 in lysosomes. NIH 3T3 cells were transfected with HA-tagged WWP2 and/or FLAG-tagged LAPTMs and cultured for 48 h. The cells were then treated with NH<sub>4</sub>Cl or H<sub>2</sub>O for 9 h and stained with  $\alpha$ -FLAG (red),  $\alpha$ -HA (green),  $\alpha$ -LAMP1 (violet), and DAPI (blue). (C and D) WWP2 degradation was inhibited by NH<sub>4</sub>Cl, a lysosome inhibitor, but not by MG132, a proteasome inhibitor. HEK293 cells transfected with HA-tagged WWP2 and/or His-tagged LAPTMs were treated with 20 mM NH<sub>4</sub>Cl or H<sub>2</sub>O for 9 h (C), or with MG132 or dimethyl sulfoxide (DMSO) for 6 h (D). Cells were then lysed and analyzed for the expression of WWP2, LAPTMs, and PTEN by immunoblot. (E) WEHI231 cells expressing LAPTMs or vector (GFP) were treated with DMSO or MG132 for 6 h and then lysed and subjected to immunoblot. (F) WWP2-mediated ubiquitination of PTEN was reduced by LAPTMs. HEK293 cells were transfected with FLAG-tagged PTEN, Myc-tagged Ub, HA-tagged WWP2, and His-tagged LAPTMs and 24 h later treated with MG132 for 6 h. The levels of PTEN ubiquitination were evaluated by immunoprecipitation of PTEN followed by anti-Ub immunoblotting. Whole-cell lysate was used as input. (G) PY motifs of LAPTMs are required for the inhibition of PTEN ubiquitination. WEHI231 cells transfected with retrovirus expressing empty vector (GFP), LAPTMs, or mutant LAPTMs for 48 h were treated with MG132 for 6 h. The levels of PTEN ubiquitination were evaluated by immunoprecipitation of PTEN followed by anti-Ub immunoblotting. (H) LAPTMs PY motifs are required for the inhibition of PTEN degradation. WEHI231 cells were transfected with retrovirus expressing empty vector, WT LAPTMs, or mutant LAPTMs with the three PY motifs mutated (mPYs) and 48 h later lysed and subjected to immunoblot. Whole-cell lysate was used as input.

undergo expansion after they arrived at the MZ. MZBs are known to have a lower threshold than FOB cells for activation and differentiation into IgM-secreting plasma cells (32, 33). In

agreement with this notion, we observed significantly elevated levels of IgM, but not IgG, anti-DNA, and anti-nuclear auto-antibodies in the serum of *Lapm5*<sup>-/-</sup>56R mice relative to

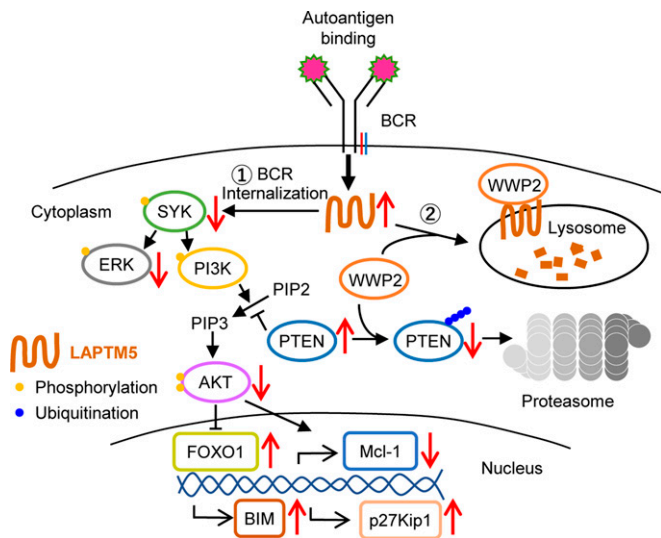


**Fig. 7.** LAPTMs5 mediates immature B cell apoptosis and maintains B cell tolerance. BCR stimulation by autoantigens up-regulates the expression of LAPTMs5, which triggers immature B cell apoptosis through two pathways that converge to suppress AKT phosphorylation. (1) LAPTMs5 causes BCR internalization, resulting in decreased phosphorylation of SYK, ERK, and possibly PI3K. This pathway is in line with the earlier findings that chronic stimulation of BM immature B cells by autoantigen results in reduced levels of p-ERK and PI3K (12, 50). (2) LAPTMs5 interacts with the E3 ubiquitin ligase WWP2 and promotes its lysosomal degradation, resulting in the accumulation of its substrate, PTEN. Elevated PTEN levels inhibit AKT phosphorylation, leading to increased FOXO1 expression and up-regulation of p27Kip1 and BIM.

56R mice, suggesting that the autoantibody-producing plasma cells might derive from  $V\kappa38C^+$  MZB cells. It should be noted that in the current study the 56R HC is in heterozygous configuration (i.e., 56R/+) both in 56R and *Lap<sup>tm5</sup><sup>-/-</sup>* 56R mice. It has been shown previously that in 56R/+ mice about 10 to 20% of the B cells expressed BCR derived from the WT allele (49), which were not enriched for editor light chains. Therefore, the effects of LAPTMs5 deficiency on the survival of autoreactive immature B and the development of  $V\kappa38C^+$  MZB cells, as well as on the production of anti-DNA antibodies, may be underestimated.

Immature B cells represent only ~15% of the B220<sup>+</sup> cells in the BM and die easily during manipulation, and are thus not suitable for exploring detailed molecular mechanisms of apoptosis. We instead used WEHI231 cells, which, similar to immature B cells in the BM, undergo apoptosis upon BCR cross-linking. Earlier studies have shown that chronic stimulation of BM immature B cells by autoantigen results in lower levels of p-ERK (50) and that BCR ligation of BM immature B cells causes reduced PIP3 levels and diminished PLC $\gamma$ 2 activation (11). The decreased levels of p-SYK, p-ERK, and p-AKT in WEHI231 cells following BCR cross-linking are in agreement with these earlier observations in BM immature B cells. Several lines of evidence indicate that LAPTMs5 is a physiological mediator of BCR-triggered immature B cell apoptosis. First, BCR stimulation up-regulated LAPTMs5 protein levels in WEHI231 cells. Second, similar to  $\alpha$ -IgM stimulation, ectopic LAPTMs5 expression induced cell cycle arrest followed by apoptosis of WEHI231 cells. Third, disruption of the *Lap<sup>tm5</sup>* gene in primary B cells and WEHI231 cells significantly suppressed the apoptosis triggered by BCR cross-linking. Fourth, ectopic LAPTMs5 expression induced signaling events that recapitulated those elicited by BCR cross-linking. However, since the proportion of apoptotic cells induced by ectopic LAPTMs5 expression was lower than that induced by BCR cross-linking and the disruption of the *Lap<sup>tm5</sup>* gene did not completely abolish BCR-triggered apoptosis, we think that

LAPTMs5 contributes to the apoptosis of some, but not all, immature B cells and that there exists a LAPTMs5-independent pathway for BCR-triggered immature B cell apoptosis.

LC-MS/MS and quantification by 4D label-free proteomics identified the E3 ubiquitin ligase WWP2 as a potential target of LAPTMs5. Subsequent biochemical experiments revealed that LAPTMs5 interacted with WWP2 and promoted its lysosomal degradation. WWP2 has previously been shown to target PTEN for ubiquitination and proteasomal degradation (41). These observations and additional analysis allowed us to uncover the molecular cascade of LAPTMs5-mediated up-regulation of PTEN. Along with our finding that LAPTMs5 protein expression was up-regulated upon BCR stimulation, the present study has revealed a previously unidentified BCR-LAPTMs5-WWP2-PTEN-p-AKT pathway that promotes cell cycle arrest and apoptosis of immature B cells and contributes to B cell tolerance (Fig. 7). Our findings are consistent with a previous study showing that BCR-mediated apoptosis of immature B cells is dependent on PTEN (13) and a more recent study showing that autoreactive B cells physiologically dampen the activity of the PI3K-AKT pathway via increasing the expression of PTEN (51). In addition, it was shown that a c-Myc/miR17-92/PTEN axis controls PI3K signals in immature B cells (12). It remains to be determined how LAPTMs5 is involved in these previously identified pathways.

LAPTMs5 is preferentially expressed in hematopoietic cells (26, 27). While biochemical and molecular data obtained with LAPTMs5-deficient and -overexpressing WEHI231 cells clearly indicated a role for LAPTMs5 in regulating BCR signaling and B cell apoptosis, the possibility remains that under *in vivo* conditions LAPTMs5 deficiency in other cell types might directly or indirectly affect the response of immature B cells. Further studies using B cell-specific deletion of the *Lap<sup>tm5</sup>* gene are required to validate the B cell-intrinsic role for LAPTMs5 in immature B cell apoptosis.

Ectopic LAPTMs5 expression down-modulated BCR levels and induced apoptosis in WEHI231 immature B cells. Our earlier studies revealed that LAPTMs5 reduced the surface BCR levels in mature B cells as a mechanism to prevent their excessive activation. Therefore, LAPTMs5 down-modulates BCR expression in both immature B and mature B cells, but the biological outcome is different, with immature B cells undergoing apoptosis while mature B cells being prevented from further activation. It has been shown that engagement of the BCR on self-reactive immature B cells leads to internalization of BCR and reduction of PI3K/AKT signaling (51). By contrast, BCR ligation in mature B cells initiates activation of the PI3K/AKT pathway and up-regulation of cell cycle proteins such as cyclin E. In addition, the PTEN level is lower in mature B cells than in immature B cells (13). Therefore, it seems that the balance between PTEN and PI3K/AKT is one of the key elements that determine the fate of immature and mature B cells after BCR stimulation. The present study reveals a previously unidentified pathway leading to immature B cell apoptosis and provides an important clue for further dissecting the molecular mechanism of opposing responses to antigen stimulation by immature vs. mature B cells.

## Materials and Methods

LAPTMs5-deficient and 56R mice have been described previously (26, 27). CRISPR-CAS9-mediated genome editing was performed as described (52). For single-cell RNA sequencing, purified BM B220<sup>+</sup> cells were processed using the 10 $\times$  Genomic Chromium Single Cell Platform. For LC-MS/MS, WEHI231 cells expressing LAPTMs5 or vector (GFP) were submitted for 4D label-free proteomics analysis. Detailed protocols for these and additional experiments are described in *SI Appendix*.

**Data, Materials, and Software Availability.** Single-cell RNA sequencing data have been deposited in the National Center for Biotechnology Information (NCBI) Gene Expression Omnibus (GEO) (56R; Laptm5KO 56R) ([GSE199926](https://www.ncbi.nlm.nih.gov/geo/query/acc.cgi?acc=GSE199926)) (53). Other data and materials from this study are available in the [SI Appendix](#), and 4D label-free data from Fig. 5 in [Dataset S1](#).

**ACKNOWLEDGMENTS.** We thank Lumin Zhang for excellent technical assistance, Dapeng Yan for providing the PCDNA3.0 ubiquitin vector, the Fudan

University animal facility for maintaining the mice, and the members in the Department of Immunology for helpful discussions.

This work was supported by the Major Research Plan of the National Natural Science Foundation of China (grant no. 91942302), the National Key R & D Plan of the Ministry of Science and Technology (grant no. 2019YFE0100600), the National Natural Science Foundation of China (grant no. 31870898), and Projects of International Cooperation and Exchanges of the National Natural Science Foundation of China (grant no. 82011540008).

1. R. Pelanda, R. M. Torres, Central B-cell tolerance: Where selection begins. *Cold Spring Harb. Perspect. Biol.* **4**, a007146 (2012).
2. F. Melchers, Checkpoints that control B cell development. *J. Clin. Invest.* **125**, 2203–2210 (2015).
3. D. Nemazee, Mechanisms of central tolerance for B cells. *Nat. Rev. Immunol.* **17**, 281–294 (2017).
4. Y. Wang, J. Liu, P. D. Burrows, J. Y. Wang, B cell development and maturation. *Adv. Exp. Med. Biol.* **1254**, 1–22 (2020).
5. T. Tsubata, B-cell tolerance and autoimmunity. *F1000 Res.* **6**, 391 (2017).
6. I. R. Mackay, N. V. Leskovek, N. R. Rose, Cell damage and autoimmunity: A critical appraisal. *J. Autoimmun.* **30**, 5–11 (2008).
7. T. K. Nowling, G. S. Gilkeson, Mechanisms of tissue injury in lupus nephritis. *Arthritis Res. Ther.* **13**, 250 (2011).
8. J. Lang *et al.*, Enforced Bcl-2 expression inhibits antigen-mediated clonal elimination of peripheral B cells in an antigen dose-dependent manner and promotes receptor editing in autoreactive, immature B cells. *J. Exp. Med.* **186**, 1513–1522 (1997).
9. S. A. Greaves, J. N. Peterson, P. Strauch, R. M. Torres, R. Pelanda, Active PI3K abrogates central tolerance in high-avidity autoreactive B cells. *J. Exp. Med.* **216**, 1135–1153 (2019).
10. M. Llorian, Z. Stamataki, S. Hill, M. Turner, I. L. Mårtensson, The PI3K p110delta is required for down-regulation of RAG expression in immature B cells. *J. Immunol. (Baltimore, MD: 1950)* **178**, 1981–1985 (2007).
11. L. Verkoczy *et al.*, Basal B cell receptor-directed phosphatidylinositol 3-kinase signaling turns off RAGs and promotes B cell-positive selection. *J. Immunol. (Baltimore, MD: 1950)* **178**, 6332–6341 (2007).
12. D. Benhamou *et al.*, A c-Myc/miR17-92/Pten axis controls PI3K-mediated positive and negative selection in B cell development and reconstitutes CD19 deficiency. *Cell Rep.* **16**, 419–431 (2016).
13. S. Cheng *et al.*, BCR-mediated apoptosis associated with negative selection of immature B cells is selectively dependent on Pten. *Cell Res.* **19**, 196–207 (2009).
14. M. Kuraoka *et al.*, Activation-induced cytidine deaminase mediates central tolerance in B cells. *Proc. Natl. Acad. Sci. U.S.A.* **108**, 11560–11565 (2011).
15. A. Gonzalez-Martin *et al.*, The microRNA miR-148a functions as a critical regulator of B cell tolerance and autoimmunity. *Nat. Immunol.* **17**, 433–440 (2016).
16. D. Nemazee, K. Buerki, Clonal deletion of autoreactive B lymphocytes in bone marrow chimeras. *Proc. Natl. Acad. Sci. U.S.A.* **86**, 8039–8043 (1989).
17. D. A. Nemazee, K. Bürki, Clonal deletion of B lymphocytes in a transgenic mouse bearing anti-MHC class I antibody genes. *Nature* **337**, 562–566 (1989).
18. R. Brink *et al.*, BCR-mediated apoptosis associated with negative selection of immature B cells is selectively dependent on Pten. *Cell Res.* **19**, 196–207 (2009).
19. M. Z. Radic *et al.*, Residues that mediate DNA binding of autoimmune antibodies. *J. Immunol. (Baltimore, MD: 1950)* **150**, 4966–4977 (1993).
20. H. Li, Y. Jiang, E. L. Prak, M. Radic, M. Weigert, Editors and editing of anti-DNA receptors. *Immunity* **15**, 947–957 (2001).
21. D. R. Sekiguchi *et al.*, Development and selection of edited B cells in B6.56R mice. *J. Immunol. (Baltimore, MD: 1950)* **176**, 6879–6887 (2006).
22. C. N. Adra *et al.*, LAPTMS: A novel lysosomal-associated multispinning membrane protein preferentially expressed in hematopoietic cells. *Genomics* **35**, 328–337 (1996).
23. M. Seimiya *et al.*, Stage-specific expression of Clast6/E3/LAPTMS during B cell differentiation: Elevated expression in human B lymphomas. *Int. J. Oncol.* **22**, 301–304 (2003).
24. T. Ishihara, J. Inoue, K. I. Kozaki, I. Imoto, J. Inazawa, HECT-type ubiquitin ligase ITC targets lysosomal-associated protein multispinning transmembrane 5 (LAPTMS) and prevents LAPTMS-mediated cell death. *J. Biol. Chem.* **286**, 44086–44094 (2011).
25. Y. Pak, W. K. Glowacka, M. C. Bruce, N. Pham, D. Rotin, Transport of LAPTMS to lysosomes requires association with the ubiquitin ligase Nedd4, but not LAPTMS ubiquitination. *J. Cell Biol.* **175**, 631–645 (2006).
26. R. Ouchida *et al.*, A lysosomal protein negatively regulates surface T cell antigen receptor expression by promoting CD3zeta-chain degradation. *Immunity* **29**, 33–43 (2008).
27. R. Ouchida, T. Kurosaki, J. Y. Wang, A role for lysosomal-associated protein transmembrane 5 in the negative regulation of surface B cell receptor levels and B cell activation. *J. Immunol. (Baltimore, MD: 1950)* **185**, 294–301 (2010).
28. W. K. Glowacka, P. Alberts, R. Ouchida, J. Y. Wang, D. Rotin, LAPTMS protein is a positive regulator of proinflammatory signaling pathways in macrophages. *J. Biol. Chem.* **287**, 27691–27702 (2012).
29. Y. Kawano *et al.*, A novel mechanism for the autonomous termination of pre-B cell receptor expression via induction of lysosome-associated protein transmembrane 5. *Mol. Cell. Biol.* **32**, 4462–4471 (2012).
30. R. D. Lee *et al.*, Single-cell analysis identifies dynamic gene expression networks that govern B cell development and transformation. *Nat. Commun.* **12**, 6843 (2021).
31. K. Lühje, B. Kretschmer, B. Fleischer, M. Breloer, CD83 regulates splenic B cell maturation and peripheral B cell homeostasis. *Int. Immunol.* **20**, 949–960 (2008).
32. J. M. Dal Porto *et al.*, B cell antigen receptor signaling 101. *Mol. Immunol.* **41**, 599–613 (2004).
33. T. Kurosaki, Genetic analysis of B cell antigen receptor signaling. *Annu. Rev. Immunol.* **17**, 555–592 (1999).
34. X. Zhang, N. Tang, T. J. Hadden, A. K. Rishi, Akt, FoxO and regulation of apoptosis. *Biochim. Biophys. Acta* **1813**, 1978–1986 (2011).
35. G. Fulop, J. Gordon, D. G. Osmond, Regulation of lymphocyte production in the bone marrow. I. Turnover of small lymphocytes in mice depleted of B lymphocytes by treatment with anti-IgM antibodies. *J. Immunol. (Baltimore, MD: 1950)* **130**, 644–648 (1983).
36. J. Gordon, The B lymphocyte-depleted mouse as a tool in immunobiology. *J. Immunol. Methods* **25**, 227–238 (1979).
37. M. T. Scupoli, G. Pizzolo, Signaling pathways activated by the B-cell receptor in chronic lymphocytic leukemia. *Expert Rev. Hematol.* **5**, 341–348 (2012).
38. B. D. Manning, A. Toker, AKT/PKB signaling: Navigating the network. *Cell* **169**, 381–405 (2017).
39. J. Li *et al.*, The PTEN/MMAC1 tumor suppressor induces cell death that is rescued by the AKT/protein kinase B oncogene. *Cancer Res.* **58**, 5667–5672 (1998).
40. V. Stambolic *et al.*, Negative regulation of PKB/Akt-dependent cell survival by the tumor suppressor PTEN. *Cell* **95**, 29–39 (1998).
41. C. A. Worby, J. E. Dixon, PTEN. *Annu. Rev. Biochem.* **83**, 641–669 (2014).
42. H. Li *et al.*, WWP2 is a physiological ubiquitin ligase for phosphatase and tensin homolog (PTEN) in mice. *J. Biol. Chem.* **293**, 8886–8899 (2018).
43. S. Maddika *et al.*, WWP2 is an E3 ubiquitin ligase for PTEN. *Nat. Cell Biol.* **13**, 728–733 (2011).
44. J. C. Cambier, S. B. Gauld, K. T. Merrell, B. J. Vilen, B-cell anergy: From transgenic models to naturally occurring anergic B cells? *Nat. Rev. Immunol.* **7**, 633–643 (2007).
45. C. C. Goodnow *et al.*, Altered immunoglobulin expression and functional silencing of self-reactive B lymphocytes in transgenic mice. *J. Immunol. (Baltimore, MD: 1950)* **183**, 5442–5448 (2009).
46. A. Enders *et al.*, Loss of the pro-apoptotic BH3-only Bcl-2 family member Bim inhibits BCR stimulation-induced apoptosis and deletion of autoreactive B cells. *J. Exp. Med.* **198**, 1119–1126 (2003).
47. A. Bendelac, M. Bonneville, J. F. Kearney, Autoreactivity by design: Innate B and T lymphocytes. *Nat. Rev. Immunol.* **1**, 177–186 (2001).
48. F. Martin, J. F. Kearney, Marginal-zone B cells. *Nat. Rev. Immunol.* **2**, 323–335 (2002).
49. L. Yunk, W. Meng, P. L. Cohen, R. A. Eisenberg, E. T. Luning Prak, Antibodies in a heavy chain knock-in mouse exhibit characteristics of early heavy chain rearrangement. *J. Immunol. (Baltimore, MD: 1950)* **183**, 452–461 (2009).
50. L. S. Teodorovic *et al.*, Activation of Ras overcomes B-cell tolerance to promote differentiation of autoreactive B cells and production of autoantibodies. *Proc. Natl. Acad. Sci. U.S.A.* **111**, E2797–E2806 (2014).
51. R. Pelanda *et al.*, B-cell intrinsic and extrinsic signals that regulate central tolerance of mouse and human B cells. *Immunity* **30**, 12–26 (2009).
52. J. Liu *et al.*, Efficient induction of Ig gene hypermutation in ex vivo-activated primary B cells. *J. Immunol. (Baltimore, MD: 1950)* **199**, 3023–3030 (2017).
53. Y. Wang, J. Wang, Single-cell analysis of bone marrow B220+ cells from 56R and LAPTMS knockout (LAPTMSKO) 56R mice. GEO. <https://www.ncbi.nlm.nih.gov/geo/query/acc.cgi?acc=GSE199926>. Deposited 1 April 2022.